

# GHOSTS — Bulges, Halos, and the Resolved Stellar Outskirts of Massive Disk Galaxies

Roelof S. de Jong<sup>1</sup>, David J. Radburn-Smith<sup>1</sup>, and Jonathan N. Sick<sup>2</sup>

<sup>1</sup>STScI, 3700 San Martin Dr., Baltimore, MD 21218, USA

<sup>2</sup>Rice University, Houston, TX 77005, USA

**Abstract.** Our GHOSTS survey measures the stellar envelope properties of 14 nearby disk galaxies by imaging their resolved stellar populations with HST/ACS&WFPC2. Most of the massive galaxies in the sample ( $V_{\text{rot}} > 200$  km/s) have very extended stellar envelopes with Sérsic law profiles or  $\mu(r) \sim r^{-2.5}$  power law profiles in the outer regions. For these massive galaxies we can fit the central bulge light and the outer halo out to 30 kpc with one and the same Sérsic profile. The stellar surface density of these profiles correlate with Hubble type and bulge-to-disk ratio, suggesting that the central bulges and inner halos are created in the same process. Smaller galaxies ( $V_{\text{rot}} \sim 100$  km/s) have much smaller stellar envelopes, but depending on geometry they could still be more luminous than expected from satellite remnants in hierarchical galaxy formation models. Alternatively, they could be created by disk heating through the bombardment of small dark matter sub-halos. The halos we fit are highly flattened, with minor-over-major axis ratios  $c/a \simeq 0.4$ . The halos are somewhat more compact than hierarchical model predictions. The halos show small metallicity gradients out to 30 kpc and the massive galaxies have typical  $[\text{Fe}/\text{H}] \sim -0.8$ . We find indications of halo substructure in many galaxies, but some halos seem remarkable smooth.

**Keywords.** galaxies: bulges, galaxies: formation, galaxies: evolution, galaxies: halos, galaxies: spiral, galaxies: stellar content, galaxies: structure, galaxies: abundances

---

Hierarchical galaxy formation in a  $\Lambda$ CDM cosmology has become the standard paradigm in recent years. However, our understanding of the galaxy formation process is incomplete. Which high redshift galaxy building blocks end up in what kind of local galaxies? How much of the stellar content of the different galaxy components (bulge, thin and thick disk, stellar halo) is created in situ and how much is accreted? How does the current accretion rate compare to  $\Lambda$ CDM predictions? To address these questions we have begun the GHOSTS† Survey, using HST to perform stellar archaeology in the outskirts of 14 nearby disk galaxies (8 of which are edge-on). For more details on the GHOSTS survey see Radburn-Smith et al., in preparation.

We obtained HST/ACS observations in the F606W and F814W bands, with typically 2–3 ACS pointings along the major and minor axes of each galaxy. Our observations reach 1.5 to 2 magnitudes below the tip of the Red Giant Branch (RGB), allowing us to identify distinct features in a Color-Magnitude Diagram (CMD) that relate to stellar populations of very different ages (for details see de Jong et al. 2007). We can investigate the spatial distribution of stars in each of these features to constrain formation histories of the different galaxy components. Using this method we have already constrained models of disk truncations in NGC 4244 (de Jong et al. 2007).

† GHOSTS: Galaxy Halos, Outer disks, Substructure, Thick disks, and Star clusters

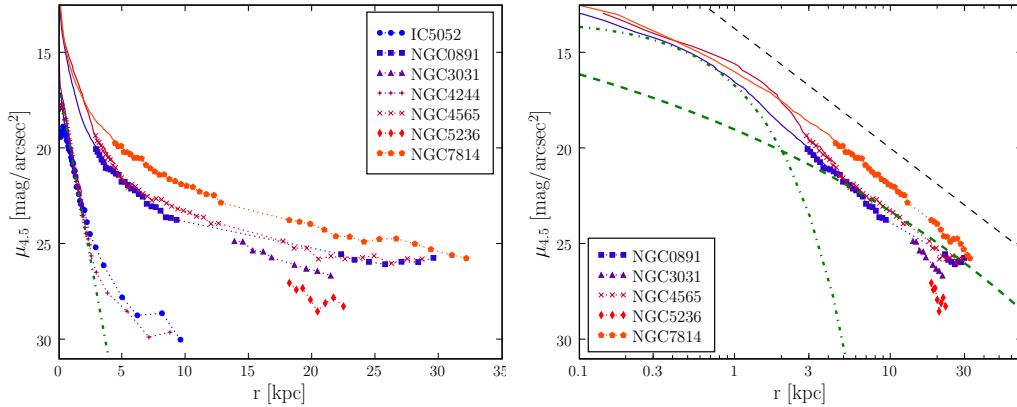


**Figure 1.** Minor axis surface density profiles of GHOSTS galaxies. The thin solid lines indicate the profiles derived from Spitzer/IRAC 4.5 micron images calibrated to Vega magnitudes (add about 3.5 mag to convert to Vega  $V$ -mag). The symbols connected with dotted lines represent RGB star count profiles, scaled to match the Spitzer data. To reduce confusion at small radii we only plot star counts beyond 12 kpc for the non-edge-on galaxies NGC 3031/M81 and NGC 5236/M83. On a linear radial scale (left diagram) exponential disks appear as straight lines, as indicated for IC5052 by the dot-dashed thick line. In the log-log plot on the right, where we have removed low mass galaxies for clarity, a straight line indicates a power law profile (e.g., thin dashed line  $= r^{-2.5}$ ). Also shown are an exponential disk (for NGC 0891, dot-dashed line) and a Sérsic profile with the typical parameters for a flattened stellar halo as modeled by Abadi et al. (2006) (thick dashed line).

## 1. Bulge and halo surface density profiles

We select RGB stars from our CMDs and use those to trace the stellar surface density. RGB stars are ideal as they are abundant in our CMDs, are indicative of old stellar populations (as expected to be found in the outskirts of galaxies), and are representative of the underlying stellar mass. To map the surface brightness profiles in the central regions of the galaxies we use the integrated light from Spitzer/IRAC 4.5 micron observations. The Spitzer images provide near unobscured light profiles, even for our edge-on galaxies. We scale the RGB surface density star counts such that they match the IR luminosity profiles in the overlapping region. In this way we derive equivalent surface brightness profiles directly from the RGB star counts.

We find that all galaxies show extended components beyond the inner exponential disk component. For the small and more face-on galaxies in the sample the size and shape of the extended component is somewhat unclear due to the uncertain contribution of contamination (unresolved background galaxies, image defects, etc.) limiting the range where the outer profile can be determined for these galaxies. Several of the most massive galaxies have very extended envelopes with stellar densities at 30 kpc that are 10–100 times higher than the contamination background, with equivalent surface brightnesses of about  $29 V\text{-mag arcsec}^{-2}$  at these radii.

In Fig. 1 we show minor-axis profiles of the edge-on galaxies analyzed so far, along with outer profiles for the more face-on galaxies NGC 3031/M81 and NGC 5236/M83. The exponential thin disks only dominate the inner  $\sim 2\text{--}3$  kpc (5–10 scale heights), while the extended components are evident at larger radii. We find that all nine galaxies analyzed thus far show components that are more extended than the exponential disks detected at small radii. Only for NGC 5236/M83 is the evidence for an extended component less certain. We measure a pure exponential disk for this galaxy to at least 20 kpc (more than 10 disk-scale lengths), but a field at 40 kpc deviates strongly from the exponential

trend. However the stellar density of this outer field is close to the sky background contamination. Furthermore, NGC 5236/M83 has at least two stellar streams at larger radii, indicating the presence of significant substructure in the halo.

### 1.1. *The bulge-halo connection*

In this section we explore the connection between bulges and the extended components.

We fit two component 2D models to the inner 4.5 micron surface brightness and outer star count data. The first component consists of a projected disk with an exponential radial profile and a *sech* vertical profile (van der Kruit 1988). The second component is a flattened halo with a Sérsic radial density profile and a minor-over-major axis ratio of  $c/a$ . Merger models show that the hot components resulting after a violent relaxation generally exhibit a Sérsic profile (e.g., Barnes & Hernquist 1992; Abadi et al. 2006, and reference therein). If bulges and stellar envelopes are created by a collisionless merger processes, we thus expect their light to follow a Sérsic profile. We show examples of the fits for a few galaxies in Fig. 2.

The profiles of the massive galaxies in our sample ( $V_{\text{rot}} > 200 \text{ km s}^{-1}$ ) can be fit entirely over a factor of 1000 in size ( $\sim 10^{4.5}$  in surface density) by an exponential disk and a single Sérsic distribution that represents both the inner bulge-like region and the outer envelope. This simple model obviously does not capture the fluctuations due to spiral arms, nor can it describe the boxy (pseudo-)bulge in edge-on galaxies NGC 891 and NGC 4565 (but does describe the central overdensity inside this boxy pseudo-bulge). The fitted models are also unable to capture the halo substructure seen as asymmetries and profile irregularities as described in the next section. The fitted halos are highly flattened, with typical  $c/a$  values of 0.4 for the edge-on galaxies.

The smaller galaxies in the sample ( $V_{\text{rot}} \simeq 100\text{--}150 \text{ km s}^{-1}$ ) have small extended components, barely discernible above the background contamination (see Fig. 1). The shape of the extended component is thus poorly constrained due to both the uncertainty in the background and low number statistics. Furthermore, the central bulge region provides no extra constraint as these galaxies have no bulge, or at most contain a central star cluster. The star counts can be fitted equally well by exponential, power law, and Sérsic law profiles. This extended feature could be the thick disk, as observations along the NGC 4244 major axis suggest the component is very flattened. However, the disk as traced by RGB stars, whose scale height is twice that of the main sequence population, has already been identified as the thick disk (Seth et al. 2005), hence the feature observed here is likely an additional component. These additional components are most likely (depending on exact shape) more luminous than predicted in the hierarchical models of Purcell et al. (2007), but could have been created by the bombardment of small dark matter sub-halos (Kazantzidis et al. 2007).

### 1.2. *Envelope properties and halo models*

Comparing the envelopes of the different galaxies we find that the two small galaxies have much smaller extended components than the larger galaxies, with surface densities that are lower relative to their disks. The more massive galaxies in our sample are very similar in terms of mass, luminosity, and scale size. Still, there is significant variation in outer envelope properties. At 20 kpc NGC 891, NGC 4565, and NGC 7814 have power law profiles with a slope of about -2.5. NGC 3031/M81 has a steeper profile, while at 20 kpc NGC 5236 is still dominated by the (face-on) disk. At first sight, the envelope luminosity at 20 kpc seems correlated with Hubble type and bulge-to-disk ratio, with the bulge dominated NGC 7814 being the brightest and the late-type spiral NGC 5236 showing only an uncertain hint of an envelope beyond 30 kpc. Whilst M31 also fits this

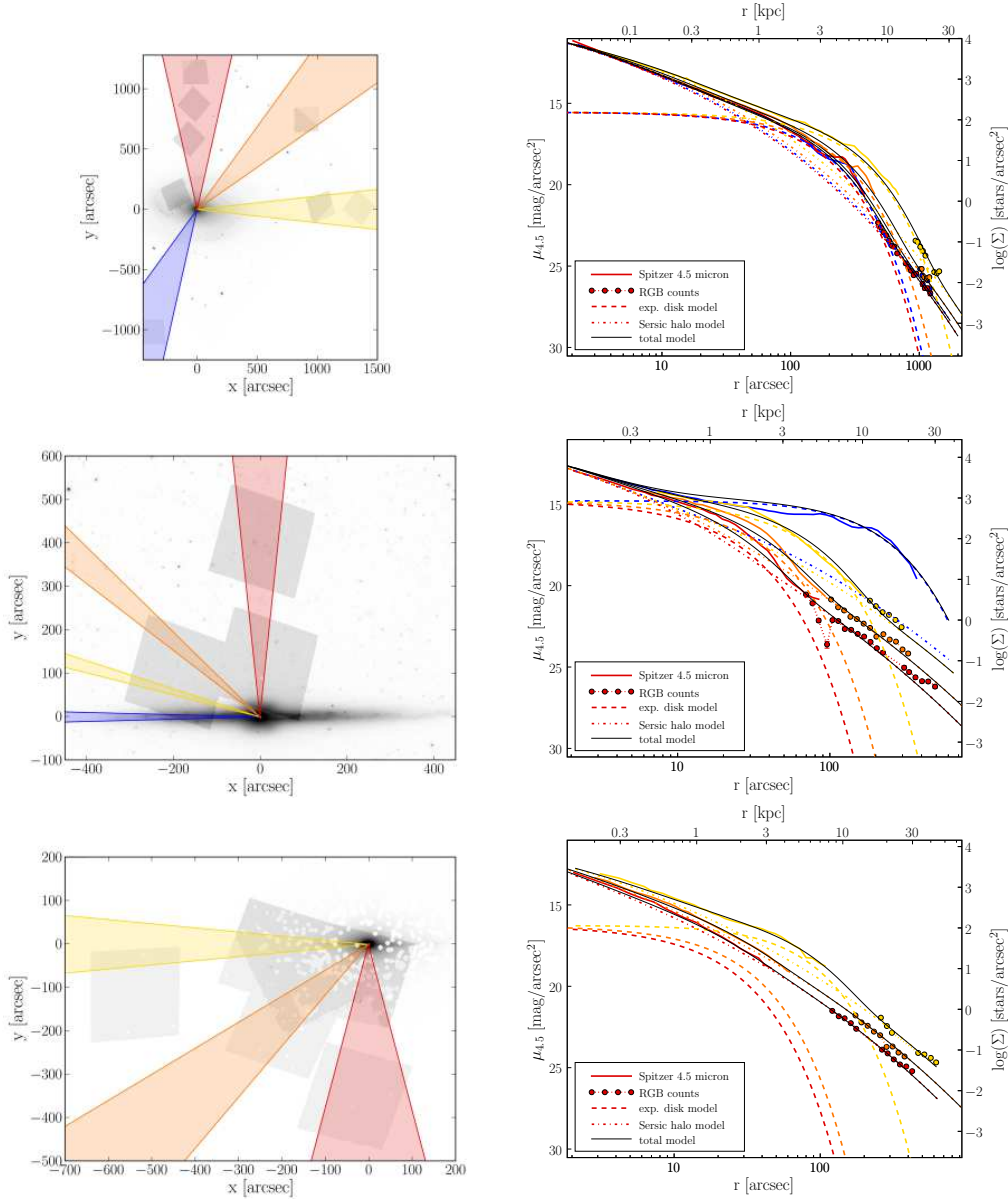


**Figure 2.** Surface density distribution and model fits of NGC 3031, NGC 4565, and NGC 7814 (top to bottom). *Left:* Gray-scale images of the *Spitzer* 4.5 micron images, with our HST/ACS footprints overlaid (shaded gray rectangular regions). The colored wedges indicate the regions used to extract the surface brightness and stellar density profiles on the right using the same color coding. *Right:* Radial *Spitzer* 4.5 micron surface brightness profiles (solid colored lines, left axis) and matched RGB stellar density profiles (points, right axis) color coded to the wedges in the diagrams to the left. The best fitting galaxy component model is shown with the exponential disk identified with long-dashed lines, the Sérsic halo with dot-dashed lines, and the combined model with thin solid lines, again color coded for the different wedges.

trend, the Sab galaxy NGC 3031/M81 does not, as a steeper and fainter profile is evident at 20 kpc on one side of the galaxy. Then again, the higher counts in another field at

20 kpc, albeit on the other side of M81, is consistent with the general trend. This observed asymmetry may be due to the multiple interactions M81 is undergoing or due to halo substructure.

In Fig. 1 we also show a typical profile from the Abadi et al. (2006) model of accreted stars. Our profiles are somewhat shallower and mostly fainter than these models between 10 and 30 kpc. While the surface density normalization may be somewhat uncertain in the models, the shape is quite well constrained. It could be that the true halos only dominate at even larger radii and the slope becomes even shallower at larger radii. However, in hierarchical galaxy formation the halo and “classical” bulge are formed by the same merging process, so there is no reason to suspect a large structural change between bulge and halo. The Sérsic radii derived for our combined envelope and bulge fits are typically eight times smaller than those of Abadi et al. (2006). However, a number of simulation parameters affect the concentration of the accreted halos. Suppressing star formation earlier, e.g. by pushing the epoch of reionization to higher redshift, ensures that only the most massive dark matter sub-halos contain stars, which yields steeper and fainter envelopes (Bekki & Chiba 2005). Alternatively, if the stars in the accreted satellites sit deeper in the potential wells of their dark matter sub-halos, they will then be tidally stripped closer to the main galaxy, also resulting in more concentrated halos (Bullock & Johnston 2005).

## 2. Halo substructure

We use Delaunay Tessellations to reconstruct the surface density distributions in our fields (Sick & de Jong, in prep.). Many galaxies show indications of halo substructure, even with our sparse sampling technique. In M83 we clearly detect a known stream that is dominated by old stars and has a metallicity  $[\text{Fe}/\text{H}] \sim -0.6$  (Seth & de Jong, in prep.). For both M81 and M83 we find significantly different surface densities on opposite sides of the galaxies at the same distance from the center. Many galaxies show deviations from smooth radial profiles, most notably NGC 891, where our outer minor axis field is much higher than expected based on an extrapolation of the inner halo profile. NGC 4631 has an obvious over-density associated with the neighboring galaxy NGC 4627 just to the north, but there is also a clear over-density to the northwest. This over-density, that is seen in main sequence, AGB, and RGB stars, is potentially associated with an HI stream in this strongly interacting system.

In stark contrast to these clear signs of substructure, we find no signs of any substructure surrounding the disk of NGC 4565. When comparing these density reconstructions with the substructure observed around M31 on the same physical scale, the NGC 4565 halo appears to be much smoother. We are currently developing techniques to quantify halo substructure.

## 3. Envelope metallicities

The metallicities of the stellar envelopes can be derived from the colors of the RGB stars, albeit with some degeneracy with population age. We have used this technique to derive the radial metallicity distribution for the GHOSTS galaxies assuming a typical population age of 10 Gyr (Fig. 3). Using younger isochrones would increase the metallicity and correcting for the AGB contamination in the RGB area will also increase the metallicity. The more massive galaxies (NGC 891, NGC 3031, NGC 4565, NGC 7814) have significantly higher metallicities than the lower mass galaxies (IC5052, NGC4244, NGC7793) as has been seen before (e.g., Mouhcine et al. 2007). Even though we detect

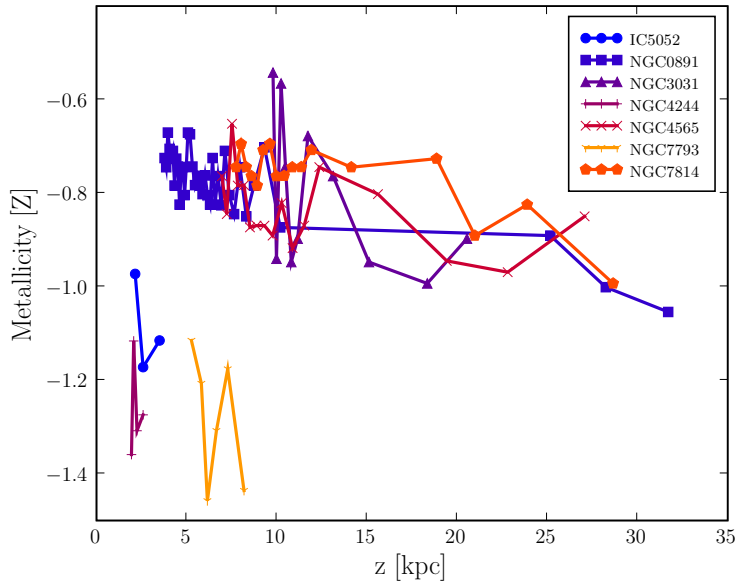


**Figure 3.** Radial minor axis metallicity profiles derived from RGB star isochrone interpolation. We used isochrones of 10 Gyr.

halo metallicity gradients for the massive galaxies, the metallicities at 30 kpc are still much higher than found for the kinematically selected Milky Way halo. We speculate that our flattened inner halos are the results of more self-enriched, massive accreted satellites, while the hotter, more metal poor halos may be detected at larger radii and are the result of earlier, less enriched, smaller satellite accretion.

### Acknowledgements

Support for Proposal numbers 9765, 10523, and 10889 was provided by NASA through a grant from the Space Telescope Science Institute, which is operated by the Association of Universities for Research in Astronomy, Incorporated, under NASA contract NAS5-26555.

### References

- Abadi, M. G., Navarro, J. F., & Steinmetz, M. 2006, MNRAS, 365, 747
- Barnes, J. E. & Hernquist, L. 1992, Ann. Rev. A&A, 30, 705
- Bekki, K. & Chiba, M. 2005, ApJL, 625, L107
- Bullock, J. S. & Johnston, K. V. 2005, ApJ, 635, 931
- de Jong, R. S. et al. 2007, ApJL, 667, L49
- Kazantzidis, S., Bullock, et al. 2007, ArXiv e-prints, 0708.1949
- Mouhcine, M., Rejkuba, M., & Ibata, R. 2007, MNRAS, 381, 873
- Purcell, C. W., Bullock, J. S., & Zentner, A. R. 2007, ApJ, 666, 20
- Seth, A. C., Dalcanton, J. J., & de Jong, R. S. 2005, AJ, 130, 1574
- van der Kruit, P. C. 1988, A&A, 192, 117